
Value Explicit Pretraining for Learning Transferable Representations

Kiran Lekkala¹ Henghui Bao¹ Sumedh Anand Sontakke¹ Laurent Itti¹

Abstract

We propose *Value Explicit Pretraining* (VEP), a method that learns generalizable representations for transfer reinforcement learning. VEP enables learning of new tasks that share similar objectives as previously learned tasks, by learning an encoder for objective-conditioned representations, irrespective of appearance changes and environment dynamics. To pre-train the encoder from a sequence of observations, we use a self-supervised contrastive loss that results in learning temporally smooth representations. VEP learns to relate states across different tasks based on the Bellman return estimate that is reflective of task progress. Experiments using a realistic navigation simulator and Atari benchmark show that the pretrained encoder produced by our method outperforms current SoTA pretraining methods on the ability to generalize to unseen tasks. VEP achieves up to a $2\times$ improvement in rewards on Atari and visual navigation, and up to a $3\times$ improvement in sample efficiency. For videos of policy performance visit our [website](#).

1. Introduction

Learning generalizable representations for control is an open problem in visual sequential decision-making. Typically, an encoder ϕ is learned using a large offline dataset via a predetermined objective function. Subsequently, ϕ is used for control by mapping high-dimensional visual observations from the environment \mathbf{o}_t into a lower-dimensional latent representation \mathbf{z}_t . The representation \mathbf{z}_t is fed into a policy $\pi(\cdot|\mathbf{z}_t)$ to generate an action \mathbf{a}_t to solve a task. The key question in visual representation learning is: *what should ϕ be?*

The challenge in learning ϕ mainly lies in discovering the correct *inductive biases* that yield representations that can be used to learn a variety of downstream tasks in a sample efficient manner.

It is unclear, however, what such useful inductive biases are. Initial approaches (Shah & Kumar, 2021; Yuan et al., 2022; Parisi et al., 2022) to this problem included simply

reusing pretrained vision models trained to solve computer vision tasks like image recognition, zero-shot for control. Subsequently, works like R3M and VIP (Nair et al., 2022; Ma et al., 2023), tried to utilize temporal consistency, enforcing that images that are temporally close in a video demonstration are embedded close to each other. Other directions include works like Voltron (Karamcheti et al., 2023) and Masked Visual Pretraining (Radosavovic et al., 2023; Xiao et al., 2022; Seo et al., 2023) which attempt to use image reconstruction as one such inductive bias.

While biases induced by pretraining objectives like image reconstruction and temporal consistency have been shown to greatly improve downstream policy performance, these pretraining objectives used to learn ϕ are *distinct* from the downstream usage of ϕ , e.g., the task of image reconstruction is very different from that of action prediction. Thus, there exists an unmet need for representation learning approaches that *explicitly* encode information directly useful for downstream control during the process of learning ϕ .

This is, of course, challenging — how do we encode control-specific information without actually training online on a control task? Our crucial insight is that encoding control-specific information in the representations generated by ϕ is possible by harnessing the power of Monte Carlo estimates of control heuristics computed offline on demonstration datasets.

Our key contribution is *Value Explicit Pretraining* (VEP), a contrastive learning approach that utilizes offline demonstration datasets with reward labels to learn a representation for visual observations. Our method utilizes the insight that observations with similar Monte Carlo Bellman return estimates across multiple tasks share a similar propensity of success and in tasks with related goals, also share a similar optimal policy. For example, in shooter games on Atari, despite differences in the visual appearances of adversaries, the strategy to effectively shoot them is similar.

VEP utilizes this intuition to learn an encoder using a contrastive loss which embeds observations with similar value function estimates across a set of training tasks near each other. We study the performance gains obtained by utilizing the VEP representation for policy learning, both on the train set of tasks and visually distinct yet related held-out tasks. We experiment on the Atari benchmark and on a vi-

sual navigation benchmark comparing VEP to state-of-the-art methods like VIP(Ma et al., 2023) and SOM(Eysenbach et al., 2022). We find up to a $2\times$ improvement in the rewards obtained on both Atari games and visual navigation and $3\times$ improvement in sample efficiency of online RL algorithms trained on VEP.

2. Related Work

Representation learning for Robotics. Besides the general idea that the representation has the role of encoding the essential information for a given task, while discarding irrelevant aspects of the original data, typical state representation learning methods attempt to embed an observation into a latent representation that could be utilized by the downstream task (Lesort et al., 2018). It is also important that these methods produce a low dimensional representation that allows the control policy to *efficiently* learn the downstream task. Traditionally, unsupervised methods like VAE (Kingma & Welling, 2014), can learn disentangled representations that can be used to correlate with observation-specific appearance factors (Higgins et al., 2017), and are used for policy learning (Ha & Schmidhuber, 2018). However, in many environments, these representations prove difficult to learn a more optimal policy, since there the temporal structure is missing in these representations. (Anand et al., 2019) explores this direction and learns representations by enforcing temporal structure through contrastive loss.

Pretraining for RL. Pretraining for representation learning, in the context of RL, involves learning transferable knowledge, typically in the form of good representations, that helps the agent perceive the world better (Xie et al., 2022). Compared with traditional unsupervised methods, the objective of pretraining for RL is to learn representations that allow efficient downstream RL. Majority of the earlier *Online pretraining* works learn representations that model the task dynamics that can be learnt through a sequence of observations during the RL procedure (Pathak et al., 2019). More recent *Offline pretraining* methods like (Schwarzer et al., 2021) build on the prior work (Anand et al., 2019) by pretraining an encoder using unlabeled data and then finetune on a small amount of task-specific data. In comparison with these approaches, our method, focuses on learning representations that not only aid solving in-domain tasks, but also is able to generalize to out-of-domain tasks (tasks that the model has not encountered, through unlabeled data).

Transfer after Pretraining. Transfer learning for reinforcement Learning is an ongoing research problem. Early works like Progressive networks (Rusu et al., 2016) attempt to solve it by reusing features learnt from source tasks through adapters. (Gamrian & Goldberg, 2019) performs

image-to-image translation using GANs. However these method are limited to predefined source or target domains. More recent works focus on a more challenging problem of using only diverse, expert videos for offline pretraining that could later be transferred to solve a downstream task. These methods have gained popularity in RL for their use of self-supervised based pretraining (Sermanet et al., 2018) based on *Contrastive Learning*. Recent works like (Eysenbach et al., 2022; Ma et al., 2023) propose methods for learning an embedding space that could be used for Zero-shot reward specification.

3. Problem setting and Preliminaries

Let $\mathcal{T}_{train} = \{\mathcal{T}_1, \mathcal{T}_2, \dots, \mathcal{T}_m\}$ be a set of train tasks, that have associated expert video demonstration datasets $\mathcal{D}_{train} = \{\mathcal{D}_1, \mathcal{D}_2, \mathcal{D}_3, \dots, \mathcal{D}_m\}$. During pretraining, we assume that the Encoder model f_ϕ parameterized by ϕ has access to \mathcal{D}_i for each of the train-tasks \mathcal{T}_{train} . Each \mathcal{D}_i consists of a sequence of frames $\{o_t^i\}$. The Encoder f_ϕ learns to encode images/observations o_t into an embedding z_t , which is taken as an input by the policy π to perform a test-task. The set of test-tasks are denoted by $\mathcal{T}_{test} = \{\mathcal{T}_{m+1}, \mathcal{T}_{m+2}, \dots, \mathcal{T}_n\}$. Note that although $\mathcal{T}_{train} \cap \mathcal{T}_{test} = \emptyset$, all the tasks in $\mathcal{T}_{train} \cup \mathcal{T}_{test}$ share a similar objective, as defined by the value function.

As our approach aims to facilitate and accelerate transfer learning for tasks with a similar objective, such similarity must be evaluated. This is an open problem in general (Zhu et al., 2023). Several methods have been proposed to quantify similarity across RL tasks (Lazarić et al., 2008). This, however, is not our primary objective here, and instead, we manually selected tasks that are intuitively similar, in two domains: 1) for urban visual-based navigation, we use maps of several cities and photographs taken along the available streets; to make tasks similar, we use a similar goal location relative to the agent’s starting point, which eliminates the need to explicitly mention goal location. 2) In Atari games, we select the shooter games, which all highly resemble the `Space Invaders` concept, albeit with graphical and other variations: an army of alien enemies descends towards the bottom of the screen, where the agent’s ship is, which can move left or right or shoot straight up.

For both our method and the baselines, the encoder f_ϕ is trained only using the expert videos $\{\mathcal{D}_1, \mathcal{D}_2, \dots, \mathcal{D}_m\}$ without any fine-tuning. The objective of our method is to efficiently learn the encoder using a sequence of observations \mathcal{D} from the source tasks \mathcal{T}_{train} , such that the embeddings from f_ϕ could be zero-shot transferred to unseen test tasks \mathcal{T}_{test} .

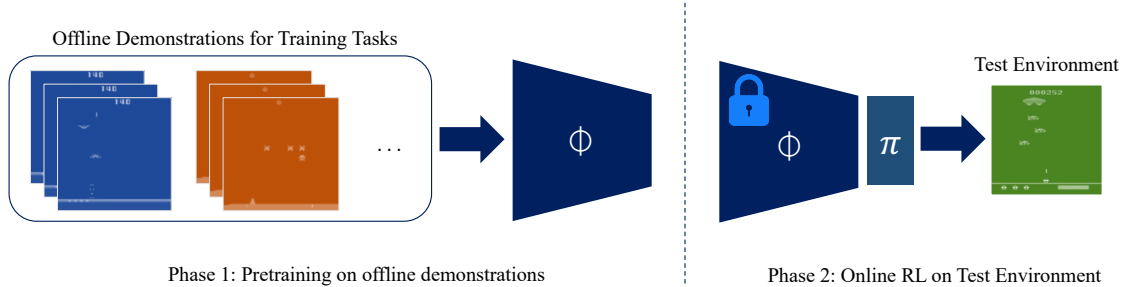


Figure 1. **High-level overview of our problem statement** The encoder f_ϕ is pretrained using expert videos from a set of train tasks, that is then reused for an unseen task. We evaluate pretrained encoders produced by our method and the baselines on the Atari and Navigation benchmarks.

3.1. Contrastive Representation Learning

Typically, contrastive representation learning methods for RL utilize offline demonstration datasets. These methods typically input a batch of anchors \mathbf{o}_{an} , positives \mathbf{o}_{ps} , and negatives \mathbf{o}_{ng} and minimize a predetermined similarity metric that enables an encoder model to learn consistent and meaningful representations that can be used for downstream tasks. The earliest known formulation (Schroff et al., 2015) uses an $\|\cdot\|_2$ distance to embed the positives and the anchor close to each other and the negatives far away from the anchor.

$$\mathcal{L}_{triplet} = \sum_{\mathbf{z} \in \mathcal{X}} \max \left[\mathbf{0}, \|\mathbf{z}_{an} - \mathbf{z}_{ps}\|_2^2 - \|\mathbf{z}_{an} - \mathbf{z}_{ng}\|_2^2 + \epsilon \right] \quad (1)$$

In the above equation \mathbf{z}_{an} , \mathbf{z}_{ps} and \mathbf{z}_{ng} represent the embeddings that are obtained after passing observations \mathbf{o}_{an} , \mathbf{o}_{ps} and \mathbf{o}_{ng} (anchors, positives and negatives) through the encoder network f_ϕ and are of shape $[B, D]$, where B is the batch size and D is the embedding size. Other metrics like cosine similarity could also be used instead of $\|\cdot\|_2$ distance, to compute the similarity between embeddings.

Similar to recent methods like (Ma et al., 2023), the InfoNCE (van den Oord et al., 2018) objective can also be used to optimize the encoder parameters. Unlike Triplet loss from Equation (1), InfoNCE permits utilizing *multiple negative examples* for calculating the loss (via to the expectation term in the denominator of Equation (2)). As depicted below, InfoNCE aims to maximize mutual information of the anchors and positives.

$$\mathcal{L}_{InfoNCE} = \mathbb{E}_{\mathbf{z}_{ps}} \left[-\log \frac{\mathcal{S}_\phi(\mathbf{z}_{an}, \mathbf{z}_{ps})}{\mathbb{E}_{\mathbf{z}_{ng}} \mathcal{S}_\phi(\mathbf{z}_{an}, \mathbf{z}_{ng})} \right] \quad (2)$$

In the above equation, \mathcal{S}_ϕ is a distance function in the ϕ -representation space that is used to compute the similarity

between a pair of embeddings. In our experiments, that use InfoNCE, \mathcal{S} takes the form of cosine similarity. More recently, Soft-Nearest Neighbor loss (Frosst et al., 2019) is a generalization of InfoNCE which also allows *multiple positive examples* (Weng, 2021) to be utilized in the computation of the objective.

$$\mathcal{L}_{SNN} = \sum_{\mathbf{z} \in \mathcal{X}} -\log \frac{\exp(-\mathcal{S}_\phi(\mathbf{z}_{an}, \mathbf{z}_{ps})/\tau)}{\exp(\mathcal{S}_\phi(\mathbf{z}_{an}, \mathbf{z}_{ng})/\tau)} \quad (3)$$

The Soft-Nearest Neighbors loss is especially useful for VEP. VEP utilizes it during a sampled batch of multiple positives (sampled from multiple training tasks from \mathcal{T}_{train}).

3.2. Discounted Returns and Value Functions

We operate using the formalism afforded by a POMDP (Partially Observable Markov Decision Process) with $(\mathcal{O}, \mathcal{S}, \mathcal{A}, p, \theta, r, T, \gamma)$ representing an observation space \mathcal{O} , state space \mathcal{S} , action space \mathcal{A} , transition function p , emission function θ , reward function r , time horizon T , and discount factor γ . An agent in state \mathbf{s}_t takes an action \mathbf{a}_t and consequently causes a transition in the environment through $p(\mathbf{s}_{t+1} | \mathbf{s}_t, \mathbf{a}_t)$. The agent receives the next state \mathbf{s}_{t+1} and reward $r_t = r(\mathbf{o}_t, \mathbf{a}_t)$ calculated using the observation \mathbf{o}_t . The goal of the agent is to learn a policy π which maximizes the expected discounted sum of rewards. The discounted sum of rewards for a sub-trajectory starting from state \mathbf{s}_t is given by:

$$G(\mathbf{s}_t) = r_{t+1} + \gamma r_{t+2} + \dots + \gamma^3 r_{t+4} = \sum_{k=t}^T \gamma^{(k-t)} r_k \quad (4)$$

The expectation of this discounted return under the trajectory distribution $p(\tau)$ and the policy π where τ is a trajec-

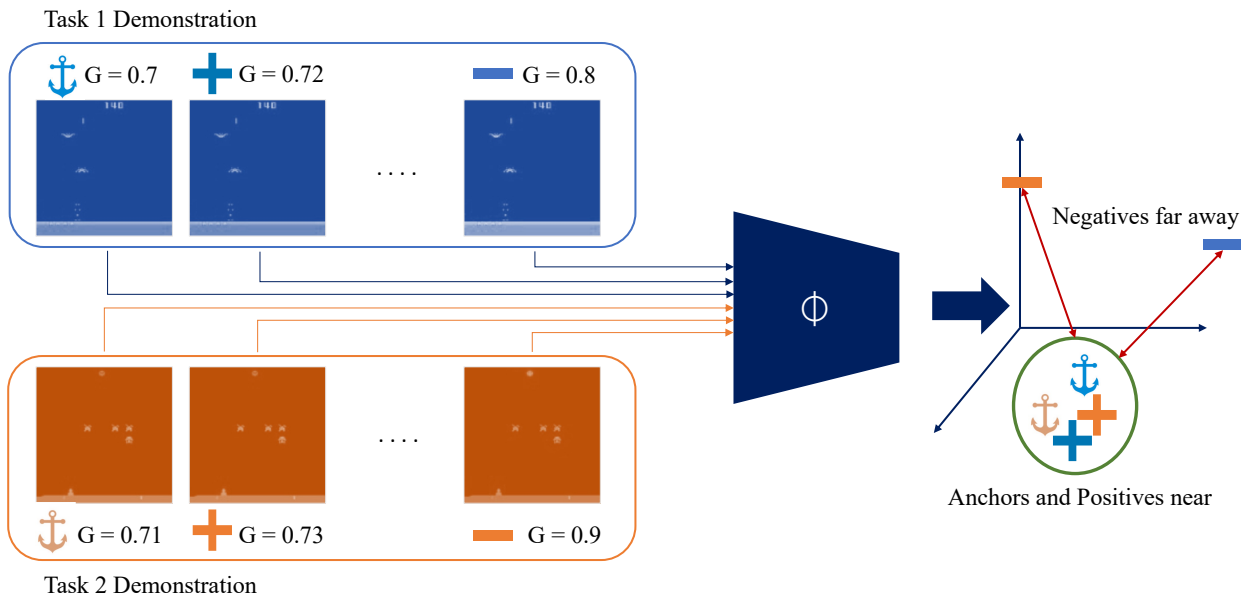


Figure 2. **Description of our method (VEP).** We compute value estimates (Bellman returns), as denoted by G , for each frame. We then use a contrastive learning-based pretraining method that learns task-agnostic representations based on G . The above figure is a pictorial representation of a training scenario where the sampling batch size b_T is 2 and the training batch size b_G is 1. This results in **anchor**, **positive** and **negative** sampled from two sequences in each batch.

tory of the form $(s_t, a_t, s_{t+1}, \dots)$ is often defined as the value of the state s_t under policy π , denoted by $\mathcal{V}^\pi(s_t)$.

4. Method

4.1. Intuition

The value $\mathcal{V}^\pi(s_t)$ of a state s_t under a policy π intuitively defines the propensity for the success of solving a task by following policy π . Intuitively, if two states have similar value estimates, they likely have a similar expected return under π .

With this in mind, we now motivate VEP with an example. Consider the task of shooting an adversary in the Atari game of Space Invaders. Assume that there exists an optimal policy for this task denoted by $\pi^*(\cdot|o_t)$ which operates on image observations and the associated optimal value function $\mathcal{V}^{\pi^*}(\cdot)$. Now, consider a slightly perturbed version of this game in which all the adversaries are colored orange. If policy π^* must solve this perturbed task, it must be invariant to the color of the adversary. One way to achieve this invariance is to enforce that the value estimates of states with similar propensities for success are similar, e.g., the value estimate of a state containing a bullet very close to an adversary should be the same regardless of whether the adversary is yellow or orange.

VEP utilizes this exact intuition by learning representations that induce such an invariance. We assume access to expert demonstrations consisting of only observations for the set of training tasks \mathcal{T}_{train} . This kind of data can be obtained from YouTube videos of gameplay or demonstration videos and does not contain any action labels. Further, it is assumed to be generated by an expert and that each of the trajectories is successful. Subsequently, we define the end of each demonstration as a goal observation o^{goal} . We also do not have access to the true reward function, so we operate under a sparse reward setting, assuming that a reward of 1 is obtained at o^{goal} and 0 everywhere else. We now label each observation with a value estimate computed using Equation (4). Ideally, this label would have been computed using $\mathcal{V}^{\pi^*}(\cdot)$, but since we do not have access to the true value function of the optimal policy, we utilize a Monte Carlo estimate of this using Equation (4).

Having labeled the demonstration datasets for tasks in \mathcal{T}_{train} with $G(\cdot)$ from Equation (4), we now train the encoder ϕ using a contrastive learning objective which first samples a scalar value estimate g between 0 and 1 and then samples multiple observations from $\mathcal{D}_1 \cup \mathcal{D}_2 \dots$ with $G(\cdot)$ values within an ϵ of g . Subsequently, an encoder ϕ is learned which embeds these observations close to each other. Consequently, observations with a similar propensity for success have similar embeddings.

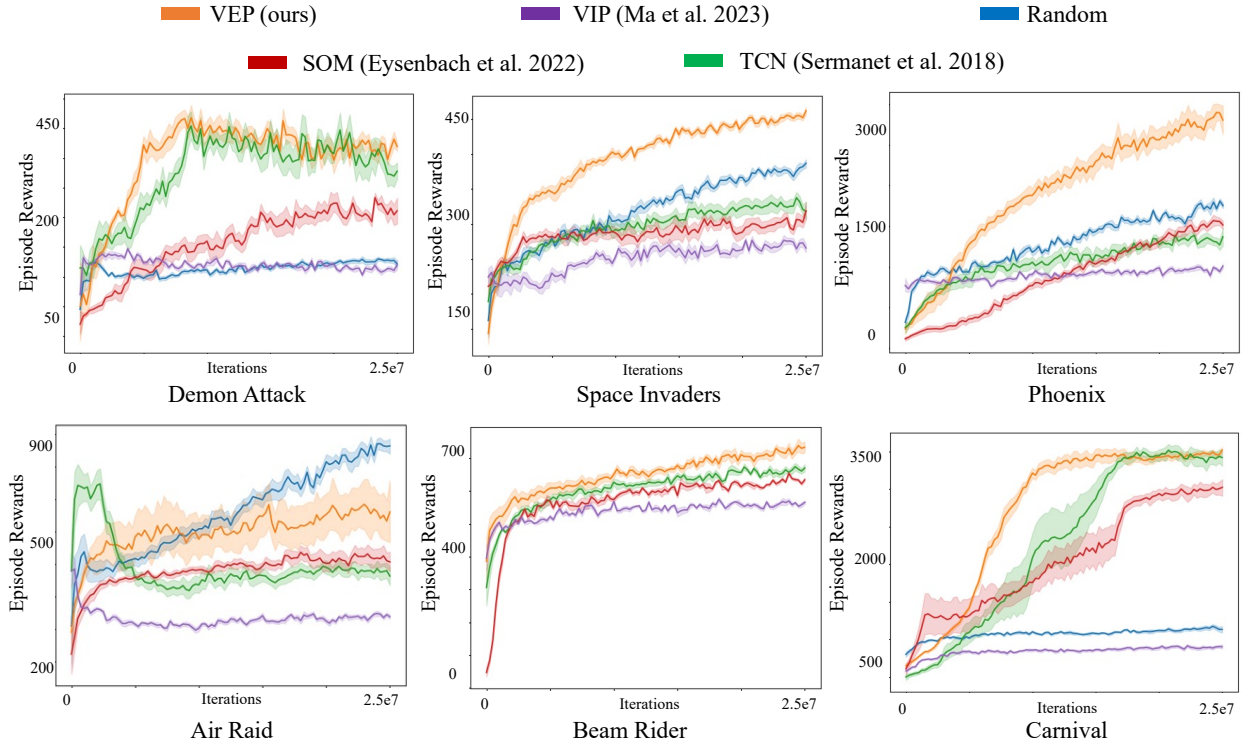


Figure 3. **Pretraining results on Atari.** Performance of different pretraining methods on the respective games as mentioned above. The encoder is pretrained only on the first 2 games (*Demon Attack* and *Space Invaders*) and is evaluated on the other out-of-domain games.

4.2. Implementation

To make the training computationally efficient, we preprocess $\mathcal{D}_1 \cup \mathcal{D}_2 \dots$ and save a dictionary that maps sorted values $G(\cdot)$ to the indices of corresponding observations with the same Monte Carlo value estimate. This speeds-up the value look-up subroutines through binary search (see supplementary material for implementation details).

We first sample a batch of value estimates from the dataset determined by train batch size b_G . Next, we sample a b_T number of training tasks. For a given value estimate and a given task, we load the observation with this value estimate as an anchor image. The positive observation corresponding to the anchor is an image with a value estimate within an ϵ of the value estimate of the anchor. In our experiments, we only sample 2 training tasks during pretraining, i.e., $b_T = 2$. Subsequently, the pretraining objective becomes the following:

$$\max_{\phi} \mathbb{E}_{g \sim [0,1]} [\mathcal{S}_{\phi}(\mathbf{z}_{an}^{\mathcal{T}_1}, \mathbf{z}_{ps}^{\mathcal{T}_1}) + \mathcal{S}_{\phi}(\mathbf{z}_{an}^{\mathcal{T}_2}, \mathbf{z}_{ps}^{\mathcal{T}_2}) + \mathcal{S}_{\phi}(\mathbf{z}_{an}^{\mathcal{T}_1}, \mathbf{z}_{ps}^{\mathcal{T}_2}) + \mathcal{S}_{\phi}(\mathbf{z}_{an}^{\mathcal{T}_2}, \mathbf{z}_{ps}^{\mathcal{T}_1})] \quad (5)$$

where g corresponds to a particular scalar value of the Bellman return estimate $G(\cdot)$. $\mathbf{z}_{an}^{\mathcal{T}_1}$ corresponds to the embedding of the anchor, i.e., observation with a value estimate equal to g sampled from task \mathcal{T}_1 , and $\mathbf{z}_{an}^{\mathcal{T}_2}$ corresponds to

the embedding of the anchor sampled from task \mathcal{T}_2 . Similarly, $\mathbf{z}_{ps}^{\mathcal{T}_1}$ corresponds to a positive, i.e., an observation with a value estimate within ϵ of g sampled from task \mathcal{T}_1 and $\mathbf{z}_{ps}^{\mathcal{T}_2}$ corresponds to a positive sampled from task \mathcal{T}_2 .

Intuitively, this objective encourages the positives and anchors from all the sampled tasks to embed near each other consequently, using the a value function estimate to organize the latent space of the learned encoder ϕ . For full implementation details like batch sizes etc., please refer to the supplementary material.

5. Experimental Setup

We study whether utilizing VEP as a pretraining objective to learn an encoder improves (1) policy learning on in-distribution tasks, i.e., those tasks for which data was available to pre-train the encoder and (2) whether the learned encoder aids transfer learning of new tasks. We performed our experiments using the benchmark specified in the next paragraph. We used the RLLib library (Liang et al., 2018) under the Ray ecosystem for all our RL experiments. We used PPO (Schulman et al., 2017) for training the policy. Additional details for our experimental setup are mentioned in the Supplementary material.

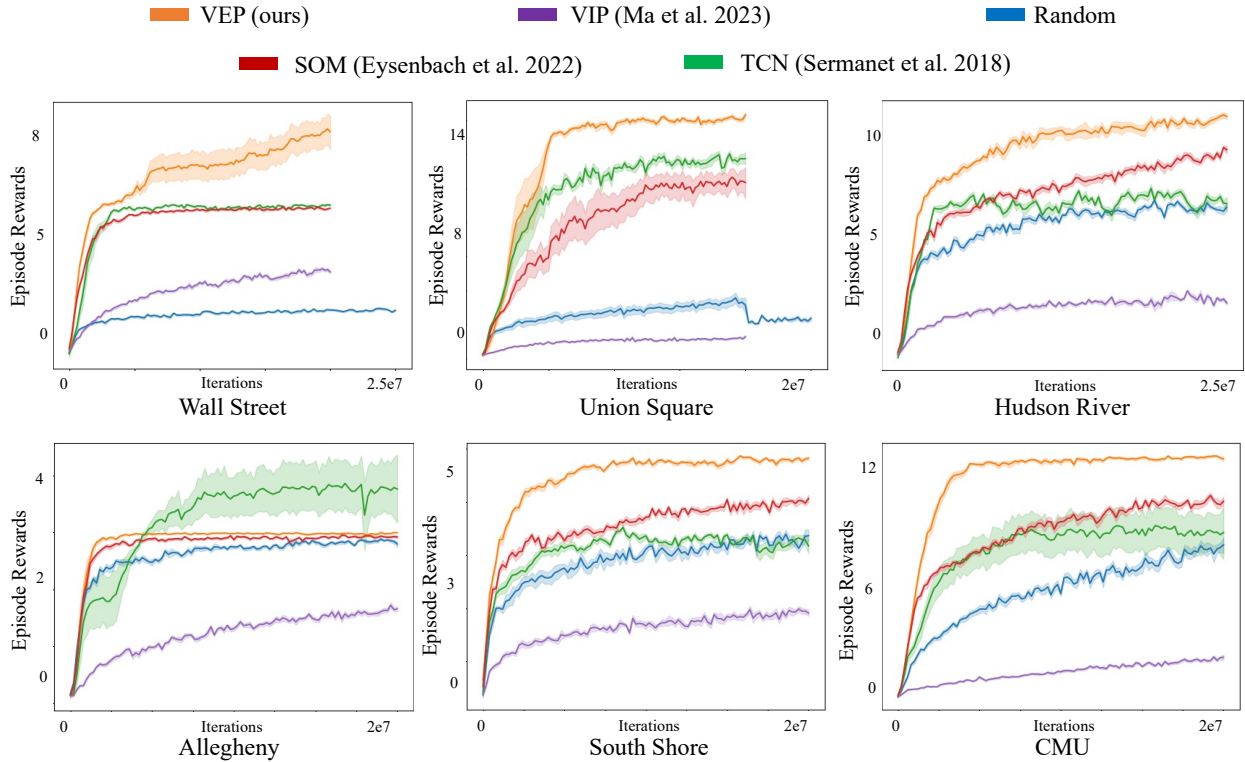


Figure 4. **Pretraining results on Navigation.** Performance of different pretraining methods on the respective cities as mentioned above. Similar to the Atari experiments, for all the baselines, expert videos from the first two tasks (*Wall Street* and *Union Square*) were used for pretraining. VEP representations improve PPO policy performance by up to $2\times$.

Algorithm 1 Value Explicit Pretraining

- Require:** $\{\mathcal{D}_i\}_{i=0}^m$ as the entire set of expert videos that are collected from tasks $\{\mathcal{T}_i\}_{i=0}^m$
- Require:** Encoder f_ϕ parameterized by ϕ
- Require:** b_G, b_T as the train and the sample batch size
- Require:** d_{thresh}, v_{thresh} as the distance and the value thresholds
- Require:** N as the number of Iterations
- 1: Randomly Initialize ϕ
 - 2: Compute value estimates G_t^i for every frame \mathbf{o}_t in the videos $\{\mathcal{D}_i\}_{i=0}^m$ with reward of the last frame as 1
 - 3: For every task \mathcal{T}_i , create a dictionary \mathbf{V}^i mapping sorted value estimates as keys to list of frame indices in $\{\mathcal{D}_i\}_{i=0}^m$
 - 4: **while** iterations until N **do**
 - 5: Sample a b_G sized batch of values $g \sim [0, 1]$
 - 6: For each g , sample a b_T sized batch of $\tau \sim \{\mathcal{T}_i\}_{i=0}^m$
 - 7: For each sampled task τ , select a frame \mathbf{o}_{an} that has a value estimate of g
 - 8: Sample a positive o_{ps} within d_{thresh}
 - 9: Mine for negatives \mathbf{o}_{ng} such that \mathbf{o}_{ng} is further away from \mathbf{o}_{an} than o_{ps}
 - 10: Estimate embeddings $\mathbf{z}_{an}, \mathbf{z}_{ps}, \mathbf{z}_{ng}$ for a batch of $\mathbf{o}_{an}, \mathbf{o}_{ps}, \mathbf{o}_{ng}$ by propagating through f_ϕ
 - 11: Compute contrastive loss using $\mathbf{z}_{an}, \mathbf{z}_{po}$ and \mathbf{z}_{ng}
 - 12: Optimize ϕ
 - 13: **end while**
-

5.1. Environments

Atari. We perform experiments by selecting a set of *Shoot'em up* games. Although all the games share a common objective of shooting enemies that spawn from above, there are significant differences in appearances and dynamics across games. We select a set of six games and split them into \mathcal{T}_{train} and \mathcal{T}_{test} . For pretraining the encoder, we use a sequence of observations obtained from the D4RL datasets (Fu et al., 2020). We truncate large sequences of raw trajectories into smaller trajectories by setting a state to terminal, when the agent gets a reward. The terminal states across all the games are unified with the objective, as all the *Shoot'em up* games deal with shooting the enemy objects. The value estimates of each frame in a sequence are then computed using Equation (4). The list of all games and the comparison across each of them is part of the supplementary material.

Navigation. We build an engine (Henghui Bao*, 2024) that loads the StreetLearn dataset (Mirowski et al., 2019) to perform visual navigation, based on gym (Brockman et al., 2016). In a typical Navigation task, the agent is designed to randomly respawn within a radius r of a predetermined location (src_x, src_y) , with the objective reaching a

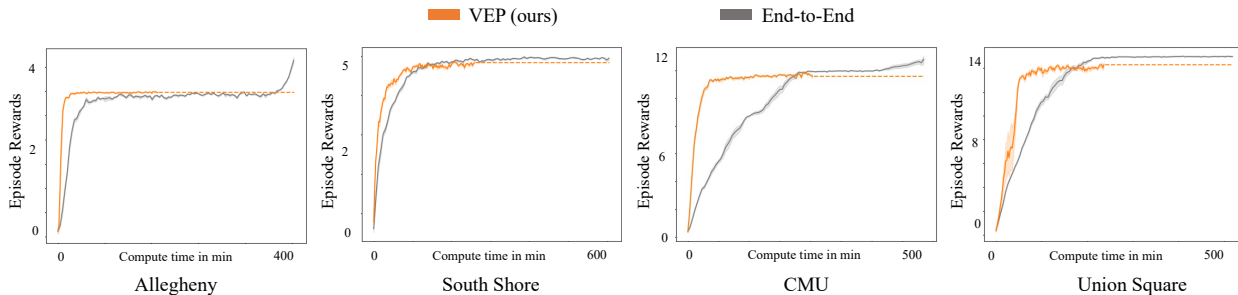


Figure 5. Comparison of our method with End-to-end trained method for Navigation task. Note that in each of the above training curves, the end-to-end baseline has the entire model trained on each of the above tasks, whereas our method (VEP) is pretrained only on expert videos from Wall Street and Union Square. Compared to any pretrained method, End-to-end training baseline takes significantly longer time ($2.1\times$ for Navigation and $3.3\times$ for Atari). Since both the methods were trained for the same number of iterations (20M), our method finished earlier and the dotted line is only for comparison

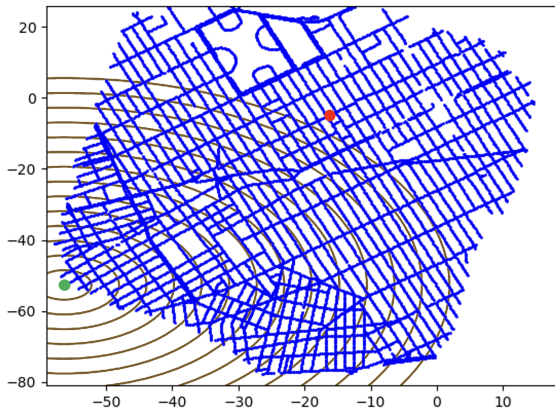


Figure 6. Reward functions for Navigation. For a specific map, the agent spawns at a predetermined starting location (red), with the flexibility to initiate at a random location within a r -step to the fixed starting point. The sparsity of the rewards (brown lines) that enable the agent to navigate to the goal (green) can be adjusted through the parameter L .

goal location that is sampled within a radius r of a location $(d_x + src_x, d_y + src_y)$. Reward acquisition is structured through a linear distribution of L reward points (including the reward obtained upon reaching the target) uniformly spanning the starting point to the goal. The agent only earns rewards as it moves closer to the goal as depicted through the yellow lines in Figure 6. We have six cities for this benchmark, and we established consistent horizontal and vertical displacements (d_x, d_y) between the starting and target points across all cities, avoiding the need for any explicit goal information (details are provided in the supplementary material). The agent is then expected to transfer to an unseen test city after learning from the expert videos obtained from a set of cities. Tasks across all the cities are all solvable within a predefined horizon. Lastly, using a planner, we obtain the expert videos by sampling all the paths under a distance limit and truncate all the paths such that the terminal state of the truncated path has a reward of 1. For all the tasks, we set $L = 15$, and $r = 5$.

We use the same encoder architecture for both Atari and Navigation to embed pixel observation into vector space. To enable temporal understanding of the state, all the embeddings in the past four timesteps are concatenated together and passed onto the policy. For the Navigation task, apart from the *four stacked* embeddings, we also obtain the subsequent *four stacked* odometry information $(odom_x, odom_y)$, of the agent, that is concatenated with the *four stacked* embedding and passed into a linear layer. This enables the agent to understand its ego-centric post that is crucial for navigating to the goal. We first pretrain the encoder f_ϕ using the method described in the previous section and visually shown in Figure 2. This is achieved by using a sequence of unlabelled trajectories from both the games. Once we obtain the pretrained encoder, we use an online RL algorithm, in our case PPO (Schulman et al., 2017), to train a policy. We summarize results in Figure 3 and Figure 4.

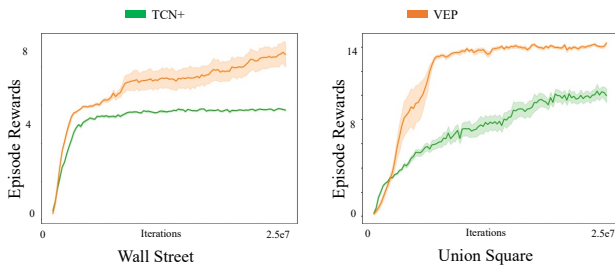


Figure 7. We compared by equating the batch size and the number of iterations to match those of VEP by combining sample and train batch size, to show that the learning ability of our method is due to value estimates amidst tasks.

5.2. Results

Baselines. *Value Implicit Pretraining (VIP)* (Ma et al., 2023) learns temporally smooth embeddings by learning by encoding the goal (positive) and the start (anchor) image

close and the middle images (negatives) within a sampled sub-trajectory. By learning this objective, through multiple sampled sub-trajectories, the encoder recursively learns continuous embeddings across sequential frames in a trajectory. *Time Contrastive Learning (TCN)* involves sampling the positive within a certain margin distance d_{thresh} from the anchor and a negative anywhere from the positive to the end of the trajectory (Sermanet et al., 2018). If the anchor is sampled at time instant t_a , positive is sampled at t_p and the negative sampled at t_n , then $|t_n - t_a| > |t_p - t_a|$. We then use the standard triplet loss for optimization, although other contrastive losses could also be used. Unlike TCN, the positives could also be sampled from *State Occupancy Measure (SOM)* (Eysenbach et al., 2022) that could be embedded close to the anchor. The negative, on the other hand, is sampled anywhere from the other episodes under a specific task or other task. State occupancy measure from a specific instant t is sampling within a truncated geometric distribution $Geo_t^H(1 - \gamma)$ with probability mass re-distributed over the interval $[t, H]$, where H is the horizon. (Mazouze et al., 2023):

Online RL experiments on Atari. For experiments involving Atari games, we trained the policy by freezing the pretrained encoder, without any additional fine-tuning. The encoder is pretrained using expert videos from *Demon Attack* and *Space Invaders*, and evaluated on a set of in-domain and out-of-domain environments. We find that the pretrained encoder is able to outperform baselines on the in-domain by ~ 25 percent. This margin is increased in the transfer experiments, most notably on *Phoenix*, with nearly $2\times$ improvement over baselines.

Online RL experiments on Navigation. Similar to the above, we froze the encoder and trained a layer policy. As mentioned before, unlike the model that was used for Atari, we also had the odometry information for a specific image that had to part of the embedding for the policy to perform the task. The embedding that was obtained from the CNN was concatenated with the 2D odometry information and was passed through another fully connected layer to obtain an embedding. All these parameters were used to pretrain. VEP outperforms all of our baselines by a larger margin in the navigation set as seen in Figure 4. VEP also outperformed the End-to-End trained baseline by achieving the same performance $2.1\times$ faster (Figure 5). We hypothesize that the better performance of our method in the Navigation tasks was due to a similar distribution of value estimate across the cities in the Navigation task, than the Atari games. Detailed specifications of the value estimates for all the Atari games and the cities in Navigation are described in the supplementary material.

Larger batch size and more iterations All the baseline approaches we compared against had a fixed train batch

size that is used for computing gradients. For VEP, we are required to use a larger batch size — $b_G \times b_T$. To ensure that gains demonstrated by VEP cannot be attributed to larger batch sizes, we doubled the batch size for TCN as seen in Figure 7. The larger batch size for TCN still does not match the performance of VEP.

Early stopping to prevent overfitting. For the Navigation task, we increased the number of training tasks. We observed that the performance degraded in this setting. As shown in Figure 8, when we reduce the number of iterations, the model retains the performance, which suggests that our method learns much faster with an increase in data diversity and early stopping can prevent overfitting.

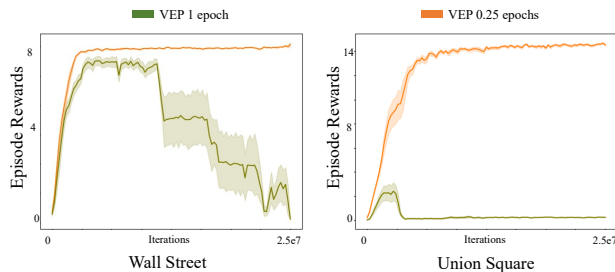


Figure 8. Comparison of our method with different early stop iterations. Notice that with an increase in number of games, our method performs better with less number of training iterations

6. Conclusion

Transferring policies to novel but related tasks is an important problem that needs to be addressed. We formulated a method to learn representations of states from different tasks solely based on the temporal distance to the goal frame. This way, the skills learnt from the train tasks could be transferred to unseen related tasks. We show the efficacy of our method by performing comprehensive evaluations on Atari and Visual Navigation.

7. Impact Statement

Our work opens new avenues for efficient training of new RL tasks by leveraging what was previously learned on similar tasks. We believe that has the potential to enable a much broader use of RL in real-life scenarios, as it eliminates the major hurdle of long and tedious training from scratch for each new task. We do not believe this work has particular ethical concerns. Its potential transformative societal impact is high as it makes RL for sequential tasks more achievable than previously possible.

References

Anand, A., Racah, E., Ozair, S., Bengio, Y., Côté, M., and Hjelm, R. D. Unsupervised state representation learning in atari. In Wallach, H. M., Larochelle, H.,

- Beygelzimer, A., d’Alché-Buc, F., Fox, E. B., and Garnett, R. (eds.), *Advances in Neural Information Processing Systems 32: Annual Conference on Neural Information Processing Systems 2019, NeurIPS 2019, December 8-14, 2019, Vancouver, BC, Canada*, pp. 8766–8779, 2019. URL <https://proceedings.neurips.cc/paper/2019/hash/6fb52e71b837628ac16539c1ff911667-Abstract.html>.
- Brockman, G., Cheung, V., Pettersson, L., Schneider, J., Schulman, J., Tang, J., and Zaremba, W. Openai gym. *CoRR*, abs/1606.01540, 2016. URL <http://arxiv.org/abs/1606.01540>.
- Eysenbach, B., Zhang, T., Levine, S., and Salakhutdinov, R. Contrastive learning as goal-conditioned reinforcement learning. In *NeurIPS*, 2022. URL http://papers.nips.cc/paper_files/paper/2022/hash/e7663e974c4ee7a2b475a4775201celf-Abstract.html.
- Frosst, N., Papernot, N., and Hinton, G. E. Analyzing and improving representations with the soft nearest neighbor loss. In Chaudhuri, K. and Salakhutdinov, R. (eds.), *Proceedings of the 36th International Conference on Machine Learning, ICML 2019, 9-15 June 2019, Long Beach, California, USA*, volume 97 of *Proceedings of Machine Learning Research*, pp. 2012–2020. PMLR, 2019. URL <http://proceedings.mlr.press/v97/frosst19a.html>.
- Fu, J., Kumar, A., Nachum, O., Tucker, G., and Levine, S. D4RL: datasets for deep data-driven reinforcement learning. *CoRR*, abs/2004.07219, 2020. URL <https://arxiv.org/abs/2004.07219>.
- Gamrian, S. and Goldberg, Y. Transfer learning for related reinforcement learning tasks via image-to-image translation. In Chaudhuri, K. and Salakhutdinov, R. (eds.), *Proceedings of the 36th International Conference on Machine Learning, ICML 2019, 9-15 June 2019, Long Beach, California, USA*, volume 97 of *Proceedings of Machine Learning Research*, pp. 2063–2072. PMLR, 2019. URL <http://proceedings.mlr.press/v97/gamrian19a.html>.
- Ha, D. and Schmidhuber, J. Recurrent world models facilitate policy evolution. In Bengio, S., Wallach, H. M., Larochelle, H., Grauman, K., Cesa-Bianchi, N., and Garnett, R. (eds.), *Advances in Neural Information Processing Systems 31: Annual Conference on Neural Information Processing Systems 2018, NeurIPS 2018, December 3-8, 2018, Montréal, Canada*, pp. 2455–2467, 2018. URL <https://proceedings.neurips.cc/paper/2018/hash/2de5d16682c3c35007e4e92982f1a2ba-Abstract.html>.
- Henghui Bao*, Kiran Lekkala*, L. I. Real world navigation in a simulator: A benchmark, 2024. URL <https://sites.google.com/usc.edu/real-world-navigation/home>.
- Higgins, I., Matthey, L., Pal, A., Burgess, C. P., Glorot, X., Botvinick, M. M., Mohamed, S., and Lerchner, A. beta-vae: Learning basic visual concepts with a constrained variational framework. In *5th International Conference on Learning Representations, ICLR 2017, Toulon, France, April 24-26, 2017, Conference Track Proceedings*. OpenReview.net, 2017. URL <https://openreview.net/forum?id=Sy2fzU9gl>.
- Karamcheti, S., Nair, S., Chen, A. S., Kollar, T., Finn, C., Sadigh, D., and Liang, P. Language-driven representation learning for robotics. *arXiv preprint arXiv:2302.12766*, 2023.
- Kingma, D. P. and Welling, M. Auto-encoding variational bayes. In Bengio, Y. and LeCun, Y. (eds.), *2nd International Conference on Learning Representations, ICLR 2014, Banff, AB, Canada, April 14-16, 2014, Conference Track Proceedings*, 2014. URL <http://arxiv.org/abs/1312.6114>.
- Lazaric, A., Restelli, M., and Bonarini, A. Transfer of samples in batch reinforcement learning. In Cohen, W. W., McCallum, A., and Roweis, S. T. (eds.), *Machine Learning, Proceedings of the Twenty-Fifth International Conference (ICML 2008), Helsinki, Finland, June 5-9, 2008*, volume 307 of *ACM International Conference Proceeding Series*, pp. 544–551. ACM, 2008. doi: 10.1145/1390156.1390225. URL <https://doi.org/10.1145/1390156.1390225>.
- Lesort, T., Rodríguez, N. D., Goudou, J., and Filliat, D. State representation learning for control: An overview. *Neural Networks*, 108:379–392, 2018. doi: 10.1016/J.NEUNET.2018.07.006. URL <https://doi.org/10.1016/j.neunet.2018.07.006>.
- Liang, E., Liaw, R., Nishihara, R., Moritz, P., Fox, R., Goldberg, K., Gonzalez, J., Jordan, M. I., and Stojica, I. Rllib: Abstractions for distributed reinforcement learning. In Dy, J. G. and Krause, A. (eds.), *Proceedings of the 35th International Conference on Machine Learning, ICML 2018, Stockholm, Sweden, July 10-15, 2018*, volume 80 of *Proceedings of Machine Learning Research*, pp. 3059–3068. PMLR, 2018. URL <http://proceedings.mlr.press/v80/liang18b.html>.

- Ma, Y. J., Sodhani, S., Jayaraman, D., Bastani, O., Kumar, V., and Zhang, A. VIP: towards universal visual reward and representation via value-implicit pre-training. In *The Eleventh International Conference on Learning Representations, ICLR 2023, Kigali, Rwanda, May 1-5, 2023*. OpenReview.net, 2023. URL <https://openreview.net/pdf?id=YJ7o2wetJ2>.
- Mazouze, B., Bruce, J., Precup, D., Fergus, R., and Anand, A. Accelerating exploration and representation learning with offline pre-training. *CoRR*, abs/2304.00046, 2023. doi: 10.48550/arXiv.2304.00046. URL <https://doi.org/10.48550/arXiv.2304.00046>.
- Mirowski, P., Banki-Horvath, A., Anderson, K., Teplyashin, D., Hermann, K. M., Malinowski, M., Grimes, M. K., Simonyan, K., Kavukcuoglu, K., Zisserman, A., and Hadsell, R. The streetlearn environment and dataset. *CoRR*, abs/1903.01292, 2019. URL <http://arxiv.org/abs/1903.01292>.
- Nair, S., Rajeswaran, A., Kumar, V., Finn, C., and Gupta, A. R3m: A universal visual representation for robot manipulation. *arXiv preprint arXiv:2203.12601*, 2022.
- Parisi, S., Rajeswaran, A., Purushwalkam, S., and Gupta, A. The unsurprising effectiveness of pre-trained vision models for control. In *International Conference on Machine Learning*, pp. 17359–17371. PMLR, 2022.
- Pathak, D., Gandhi, D., and Gupta, A. Self-supervised exploration via disagreement. In Chaudhuri, K. and Salakhutdinov, R. (eds.), *Proceedings of the 36th International Conference on Machine Learning, ICML 2019, 9-15 June 2019, Long Beach, California, USA*, volume 97 of *Proceedings of Machine Learning Research*, pp. 5062–5071. PMLR, 2019. URL <http://proceedings.mlr.press/v97/pathak19a.html>.
- Radosavovic, I., Xiao, T., James, S., Abbeel, P., Malik, J., and Darrell, T. Real-world robot learning with masked visual pre-training. In *Conference on Robot Learning*, pp. 416–426. PMLR, 2023.
- Rusu, A. A., Rabinowitz, N. C., Desjardins, G., Soyer, H., Kirkpatrick, J., Kavukcuoglu, K., Pascanu, R., and Hadsell, R. Progressive neural networks. *CoRR*, abs/1606.04671, 2016. URL <http://arxiv.org/abs/1606.04671>.
- Schroff, F., Kalenichenko, D., and Philbin, J. Facenet: A unified embedding for face recognition and clustering. In *IEEE Conference on Computer Vision and Pattern Recognition, CVPR 2015, Boston, MA, USA, June 7-12, 2015*, pp. 815–823. IEEE Computer Society, 2015. doi: 10.1109/CVPR.2015.7298682. URL <https://doi.org/10.1109/CVPR.2015.7298682>.
- Schulman, J., Wolski, F., Dhariwal, P., Radford, A., and Klimov, O. Proximal policy optimization algorithms. *CoRR*, abs/1707.06347, 2017. URL <http://arxiv.org/abs/1707.06347>.
- Schwarzer, M., Rajkumar, N., Noukhovitch, M., Anand, A., Charlin, L., Hjelm, R. D., Bachman, P., and Courville, A. C. Pretraining representations for data-efficient reinforcement learning. In Ranzato, M., Beygelzimer, A., Dauphin, Y. N., Liang, P., and Vaughan, J. W. (eds.), *Advances in Neural Information Processing Systems 34: Annual Conference on Neural Information Processing Systems 2021, NeurIPS 2021, December 6-14, 2021, virtual*, pp. 12686–12699, 2021. URL <https://proceedings.neurips.cc/paper/2021/hash/69eba34671b3ef1ef38ee85caae6b2a1-Abstract.html>.
- Seo, Y., Hafner, D., Liu, H., Liu, F., James, S., Lee, K., and Abbeel, P. Masked world models for visual control. In *Conference on Robot Learning*, pp. 1332–1344. PMLR, 2023.
- Sermanet, P., Lynch, C., Chebotar, Y., Hsu, J., Jang, E., Schaal, S., and Levine, S. Time-contrastive networks: Self-supervised learning from video. In *2018 IEEE International Conference on Robotics and Automation, ICRA 2018, Brisbane, Australia, May 21-25, 2018*, pp. 1134–1141. IEEE, 2018. doi: 10.1109/ICRA.2018.8462891. URL <https://doi.org/10.1109/ICRA.2018.8462891>.
- Shah, R. and Kumar, V. Rrl: Resnet as representation for reinforcement learning. *arXiv preprint arXiv:2107.03380*, 2021.
- van den Oord, A., Li, Y., and Vinyals, O. Representation learning with contrastive predictive coding. *CoRR*, abs/1807.03748, 2018. URL <http://arxiv.org/abs/1807.03748>.
- Weng, L. Contrastive representation learning. *lilianweng.github.io*, May 2021. URL <https://lilianweng.github.io/posts/2021-05-31-contrastive/>.
- Xiao, T., Radosavovic, I., Darrell, T., and Malik, J. Masked visual pre-training for motor control. *arXiv preprint arXiv:2203.06173*, 2022.
- Xie, Z., Lin, Z., Li, J., Li, S., and Ye, D. Pre-training in deep reinforcement learning: A survey. *CoRR*, abs/2211.03959, 2022. doi: 10.48550/ARXIV.2211.03959. URL <https://doi.org/10.48550/arXiv.2211.03959>.

Yuan, Z., Xue, Z., Yuan, B., Wang, X., Wu, Y., Gao, Y., and Xu, H. Pre-trained image encoder for generalizable visual reinforcement learning. *Advances in Neural Information Processing Systems*, 35:13022–13037, 2022.

Zhu, Z., Lin, K., Jain, A. K., and Zhou, J. Transfer learning in deep reinforcement learning: A survey. *IEEE Trans. Pattern Anal. Mach. Intell.*, 45(11):13344–13362, 2023. doi: 10.1109/TPAMI.2023.3292075. URL <https://doi.org/10.1109/TPAMI.2023.3292075>.